Desalination and Water Treatment
www.deswater.com
doi: 10.5004/dwt.2020.24904

175 (2020) 273–281
January

Removal of Orange II using an adsorbent-supported zero-valent iron as a heterogeneous Fenton-like catalyst

Jiwei Liu[a], Yufeng Du[a], Tong Ye[a], Jiangfei Cao[b], Changsheng Peng[a,b,*]

[a]*The Key Lab of Marine Environmental Science and Ecology, Ministry of Education, Ocean University of China, Qingdao 266100, China, Tel. +86 532 66782011; Fax: +86 532 66782011; emails: pcs005@ouc.edu.cn (C.S. Peng), liujiwei_zyw@163.com (J. Liu), duyfsdut@126.com (Y.F. Du), 343125088@qq.com (T. Ye)*
[b]*School of Environmental and Chemical Engineering, Zhaoqing University, Zhaoqing 526061, China, email: 903015619@qq.com*

Received 7 May 2019; Accepted 13 September 2019

ABSTRACT

Orange II was difficult to degrade and it was selected as a target pollutant in the present study. In this paper, a granular porous adsorbent (GPA) containing zero-valent iron (ZVI) (GPA-ZVI) was produced and applied as a Fenton-like oxidation catalyst to degrade Orange II. Firstly, GPA-ZVI was prepared with coke as the reducing agent, *Enteromorpha prolifera* as the pore-forming agent, iron ore tailings as a source of ZVI, fly ash as the skeletal material and bentonite as the binder. ZVI was produced through the reduction of iron ore tailings powder by coke at a high temperature under a reducing atmosphere and embedded in the granular porous-based adsorbent. Secondly, the structure and composition of the GPA-ZVI were analyzed by Brunauer–Emmett–Teller method, X-ray diffraction, energy dispersive spectroscopy, Fourier transform infrared spectrometry and scanning electron microscopy. Thirdly, batch experiments were performed to study the influence of some parameters such as GPA-ZVI dosage, H_2O_2 concentration, pH, and temperature on Orange II removal. The removal efficiency of Orange II using a combined GPA-ZVI and Fenton oxidation process (GPA-ZVI/H_2O_2) was 91.24% while the removal efficiency of Orange II by H_2O_2, GPA-ZVI and Fe^{2+}/H_2O_2 was only 1.48%, 18.94%, and 58.43%, respectively. The degradation kinetics fitted to the pseudo-first-order kinetic model. Removal mechanisms of Orange II using GPA-ZVI/H_2O_2 including the adsorption and oxidation were proposed. In a word, GPA-ZVI/H_2O_2 was highly effective in degrading Orange II.

Keywords: GPA-ZVI; Orange II; Fenton process; Oxidation; Adsorption; Reduction

1. Introduction

Orange II is an azo dye and it is widely implemented in different types of industries, which brings about a serious environmental issue because of its carcinogenesis to aquatic animals and humans [1]. Orange II mainly consists of a naphthalene ring, a benzene ring and an azo linkage [2]. Due to its stability, non-biodegradability, and carcinogenesis, researching several new-style and effective techniques to remove Orange II is an urgent need.

In recent years, various treatment methods including coagulation, flocculation, and adsorption have been researched to remove Orange II [3]. Recently, zero-valent iron (ZVI) has drawn great attention and it is widely employed in the water treatment because of high intrinsic reactivity, larger surface area, and non-toxicity. However, ZVI has a strong tendency to agglomerate and oxidize, resulting in losing its high reactivity, larger surface area, reducing power and catalytic ability [4]. To overcome this disadvantage, the utilization of supporting porous materials like biochar, reduced graphene

* Corresponding author.

oxide, zeolite, and mesoporous carbon is a promising method to solve this issue [5,6]. Also, ZVI can serve as a source of Fe^{2+}, which can activate H_2O_2 to generate hydroxyl radicals for Fenton-like oxidation of organic contaminants [7].

Fenton process is one of the most effective advanced oxidation processes and it can generate hydroxyl radicals having a strong oxidation capacity [8,9]. Fe^{2+} is used as the catalyst and hydrogen peroxide is used as the oxidant in the Fenton process. However, there are still some disadvantages such as the generation of iron sludge, the requirement of further treatment and the intermittence of the reaction cycle [10]. To address these issues, solid Fe_2O_3, Fe_3O_4, FeOOH, and ZVI as heterogeneous Fenton-like catalysts are used to treat various organic pollutants in water [11,12]. ZVI as a heterogeneous catalyst has attracted increasing attention and it is used as the source of Fe^{2+} generated from the corrosion of ZVI in acidic solution [13]. ZVI can also promote the electron transfer ($Fe^0 + Fe^{3+} \rightarrow Fe^{2+}$) on the surface of ZVI, which favors the Fenton reaction cycle [14].

In this work, ZVI was produced through the reduction of iron ore tailings powder by coke at a high temperature under a reducing atmosphere and embedded in GPA. ZVI and Fe_3O_4 existed in granular porous adsorbent (GPA) containing zero-valent iron (ZVI) (GPA-ZVI) and could provide more Fe^{2+} ions as the catalyst in the Fenton system. In addition, GPA-ZVI had various functional groups and a higher specific surface area. The removal of Orange II using GPA-ZVI/H_2O_2 was investigated. The objective of this paper is to study: (i) the preparation and characteristics of GPA-ZVI, (ii) the influence of key parameters on Orange II removal using GPA-ZVI/H_2O_2, and (iii) the removal mechanisms of Orange II using GPA-ZVI/H_2O_2 [15].

2. Experimental setup

2.1. Materials and chemicals

Orange II ($C_{16}H_{11}N_2NaO_4S$), hydrogen peroxide (H_2O_2), sodium hydroxide (NaOH), potassium permanganate ($K_2Cr_2O_7$), phosphoric acid (H_3PO_4), ferric chloride hexahydrate ($FeCl_3{\cdot}6H_2O$), sulphuric acid (H_2SO_4), methylene blue ($C_{16}H_{18}ClN_3S$), hydrochloric acid (HCl), and sodium diphenylamine sulfonate ($C_{16}H_{18}NNaO_3S$) were obtained from Sinopharm Chemical Reagent (Shanghai, China). Bentonite, *Enteromorpha prolifera*, fly ash, coke and iron ore tailings were supplied from Qingdao, China. A stock solution of Orange II (1,000 mg L^{-1}) was prepared via dissolving Orange II in deionized water.

2.2. Preparation of GPA-ZVI

Bentonite, *Enteromorpha prolifera*, fly ash, coke, and iron ore tailings were initially dried at 65°C for 24 h. Subsequently, they were ground in an agate mortar for 12 h by a three-head grinding machine and passed into 200-mesh sieves. First, raw materials with an iron ore tailings/coke/fly ash/bentonite mass ratio of 2:2:2:1 were mixed in a mixer with 1 wt.% *Enteromorpha prolifera* and 10 wt.% distilled water. Next, the mixtures were formed to the particles by pressing with a granulator. Finally, after dried at 105°C for 24 h, the materials were heated in a furnace at 900°C with a heating rate of 10°C min^{-1} for 90 min under a reducing atmosphere and cooled in a vacuum [16]. Schematic procedure of the synthesis of GPA-ZVI is illustrated in Fig. S1.

2.3. Characterization techniques

The morphologies of GPA-ZVI was investigated using a scanning electron microscopy (SEM, JSM-6700F), followed by an analysis of the chemical composition using energy dispersive spectroscopy (EDS, JSM-6700F). The functional groups of GPA-ZVI before and after reactions were identified using Fourier transform infrared spectroscopy (FTIR, Bruker Vertex 70, Germany). The Brunauer–Emmett–Teller (BET)-N_2 adsorption method was used to test the specific surface area with a surface analyzer (Micromeritics, ASAP 2020). X-ray Diffraction spectroscopy patterns of GPA-ZVI were performed using a diffractometer (XRD, D/max-γB).

2.4. Removal experiments

To evaluate the degradation performance of H_2O_2, GPA-ZVI, Fe^{2+}/H_2O_2 and GPA-ZVI/H_2O_2 in Fenton system, the removal of Orange II using H_2O_2, GPA-ZVI, Fe^{2+}/H_2O_2 and GPA-ZVI/H_2O_2 was carried out by adding Fe^{2+} (100 mg L^{-1}), GPA-ZVI (0.20 g) and H_2O_2 (50 mM) into 100 mL Orange II solution (1,000 mg L^{-1}) at pH 3, temperature 303 K and 120 rpm for 72 h. The effects of the initial pH (1~7), GPA-ZVI dosage (0.01~1.20 g), H_2O_2 concentration (10~900 mM) and temperature (293~323 K) on Orange II removal by GPA-ZVI/H_2O_2 were investigated. The determination of the Orange II concentration in the solution was obtained at λ_{max} = 484 nm in the UV-vis spectrophotometer. The removal capacity and efficiency of Orange II were calculated by Eqs. (1) and (2).

$$q_t = \frac{\left(C_0 - C_t\right) \times V}{w} \tag{1}$$

$$R(\%) = \frac{\left(C_0 - C_t\right)}{C_0} \times 100 \tag{2}$$

Here q_t (mg g^{-1}) is the removal capacity of Orange II, C_0 (mg L^{-1}) is the concentration of Orange II at initial time, V (L) is the volume, R (%) is the removal efficiency of Orange II, C_t (mg g^{-1}) is the concentration of Orange II at time t, w (g) is the weight.

3. Results and discussion

3.1. Characterization of GPA-ZVI

The surface morphology structures of GPA-ZVI was investigated by SEM and EDS analysis as presented in Figs. S2a and b. As shown in Fig. S2a, it is clear that many pores existed in GPA-ZVI, which was ascribed to the pyrolysis of the pore-forming agent (*Enteromorpha prolifera*) and the reducing agent (coke) [17]. Moreover, the size of the iron ore tailings powder diminished during sintering, which resulted in forming a number of pores in GPA-ZVI. This also proved that GPA-ZVI was a porous adsorbent. In addition, the SEM image of GPA-ZVI displays spherical

iron particles with a size ranged from several nanometers to several microns. The EDS image shows that Fe, Al, Si, O, and C were the main elements in GPA-ZVI (Fig. S2b).

The XRD pattern of GPA-ZVI demonstrates the presence of ZVI (2θ = 44.64°) (Fig. S2c) [18]. Meanwhile, this also confirmed that iron oxide was reduced to ZVI by coke. In addition, ZVI was embedded and evenly dispersed in the porous adsorbent. The content of ZVI in GPA-ZVI was measured to be 41.94 mg g^{-1}.

The FTIR spectra for GPA-ZVI before and after reactions were recorded and the results are shown in Fig. S2d. The characteristic band was observed at 3,400 cm^{-1} that was attributed to OH. The broad absorption bands at 1,620 and 1,420 cm^{-1} were attributed to COOH. The peaks were observed at 561 and 469 cm^{-1} that were attributed to Fe–O of Fe_2O_3 and Fe_3O_4. The changes of the peaks at 561 and 469 cm^{-1} were observed, indicating that Fe^0 was oxidized to Fe^{2+} or Fe^{3+} after the Orange II removal experiment [19].

To investigate the pore size distribution and specific surface area, BET analysis was used as shown in Figs. S2e and f. The nitrogen adsorption–desorption isotherms for GPA-ZVI are of a typical type IV with a type H1 hysteresis loop caused by the mesoporous pores of GPA-ZVI, which was according to the International Union of Pure and Applied Chemistry (IUPAC) classification. The Barrett–Joyner–Halenda (BJH) pore size distribution carve indicates that GPA-ZVI had a mesoporous structure. According to the results, the average pore size and BET surface area were measured to be 6.26 nm and 14.09 m^2 g^{-1}, respectively, which indicated that GPA-ZVI had a relatively higher porosity.

3.2. Comparison of various processes for removing Orange II

The removal of Orange II by H_2O_2 alone, GPA-ZVI alone, Fe^{2+}/H_2O_2 and GPA-ZVI/H_2O_2 were investigated as presented in Fig. 1. When using H_2O_2, GPA-ZVI, Fe^{2+}/H_2O_2 and GPA-ZVI/H_2O_2 for removing Orange II, the removal efficiency by H_2O_2 alone, GPA-ZVI alone, Fe^{2+}/H_2O_2 and GPA-ZVI/H_2O_2 was 1.48%, 18.94%, 58.43%, and 91.24%, respectively.

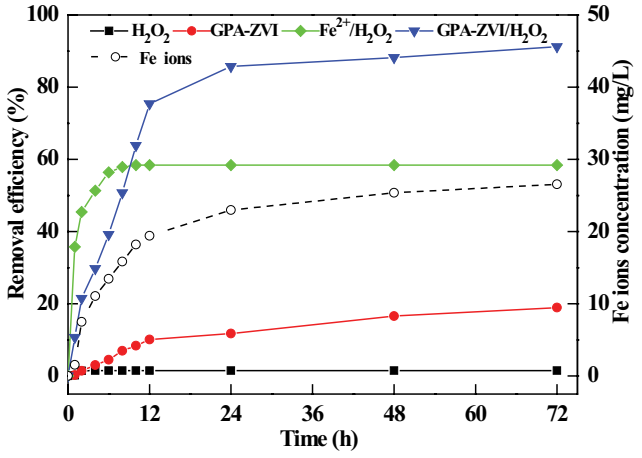

Fig. 1. Removal of Orange II using H_2O_2, GPA-ZVI, Fe^{2+}/H_2O_2 and GPA-ZVI/H_2O_2 (Initial Orange II concentration 1,000 mg L^{-1}, H_2O_2 concentration 50 mM, GPA-ZVI dosage 2 g L^{-1}, Fe^{2+} concentration 100 mg L^{-1}, pH 3, temperature 303 K).

The removal capacity of Orange II was 456.19 mg g^{-1} for GPA-ZVI/H_2O_2 and 94.70 mg g^{-1} for GPA-ZVI. By comparison of the removal efficiency of Orange II by H_2O_2, GPA-ZVI and Fe^{2+}/H_2O_2, the removal efficiency of Orange II by GPA-ZVI/H_2O_2 was higher than that by three other processes, confirming that the removal of Orange II by GPA-ZVI/H_2O_2 was more effective than that by H_2O_2, GPA-ZVI and Fe^{2+}/H_2O_2. This was because that (i) the oxidizability of H_2O_2 without Fe^{2+} as a catalyst for Orange II degradation was too weak [15], (ii) Orange II could be removed by GPA-ZVI but the removal efficiency was lower, and (iii) the removal of Orange II using GPA-ZVI/H_2O_2 was effective [20,21]. In addition, by comparison of the removal of Orange II in various Fenton processes according to the previous literature (Table 1), GPA-ZVI/H_2O_2 showed highly efficient for Orange II removal. Furthermore, Fe ions concentration increased in GPA-ZVI/H_2O_2 system with the increase of reaction times (Fig. 1). However, Fe ions concentration was lower at equilibrium time, which may be ascribed to the fact that Fe^{3+} was absorbed in the inner pores or onto the surface of GPA-ZVI.

3.3. Effect of experimental parameters on the removal of Orange II by GPA-ZVI/H_2O_2

The pH plays a vital role in the removal process of Orange II, which affects the solubility of Fe^{2+}/Fe^{3+} and the production of hydroxyl radicals [28]. The influence of pH on Orange II removal by GPA-ZVI/H_2O_2 was investigated by varying pH from 1.0 to 7.0 as shown in Fig. 2. The removal efficiency of Orange II by GPA-ZVI/H_2O_2 increased with the pH value decreased, indicating that GPA-ZVI coupled with H_2O_2 was more effective in the removal of Orange II at lower pH [29]. This was because the acidic condition was favorable to the corrosion of Fe^0, which produced more Fe^{2+}. Moreover, the reaction between Orange II and GPA-ZVI/H_2O_2 occurred easily and the removal rate was rapid at lower pH value. A low pH value was conducive to reconvert Fe^{3+} to Fe^{2+}, which made the reaction recyclable [30]. Furthermore, at lower pH, the negatively charged Orange II was easily absorbed onto the positively charged surface of GPA-ZVI whose functional groups such as OH and COOH were easily protonated by H^+ under acidic conditions. In addition, Fe^{3+} formed the precipitation of $Fe(OH)_3$ and H_2O_2 was decomposed to O_2 at higher pH value, leading to the deactivation of catalyst and the decrease in Orange II removal [31]. As shown in Fig. 2, the leaching Fe ions concentration increased as initial pH decreased. In addition, the final pH of the solutions slightly increased, which was attributed to the consumption of H^+.

The availability of Fe^{2+} plays a major role in the production of hydroxyl radicals, determining the degradation performance of GPA-ZVI/H_2O_2. The effect of the GPA-ZVI dose in the range of 0.01~1.20 g on Orange II removal by GPA-ZVI/H_2O_2 was analyzed as indicated in Fig. 3. It shows that the removal efficiency of Orange II increased with increasing the dose of GPA-ZVI ranged from 0.01 to 0.20 g. This was becuase increasing the GPA-ZVI dose increased the surface sites, specific surface area and the amount of released Fe^{2+} catalyst, which enhanced the removal efficiency of Orange II. In addition, Fig. 3 shows that the removal efficiency decreased with the increase in the dose of GPA-ZVI from

Table 1
Removal of Orange II in various Fenton processes

Catalyst	Conditions	R (%)	q_m (mg g^{-1})	References
GPA-ZVI	Dosage: 2 g L^{-1}; H_2O_2: 50 mM; pH: 3; Orange II: 1,000 mg L^{-1} (100 mL); 30°C	91	456.19	This work
Nanoscale zero-valent iron	Dosage: 20 mg L^{-1}; H_2O_2: 200 mg L^{-1}; pH: 3; Orange II: 105 mg L^{-1} (1 L); 25°C	100	52.50	[22]
$Fe_2(MoO_4)_3$	Dosage: 1.4 g L^{-1}; H_2O_2: 18 mM; pH: 3; Orange II: 100 mg L^{-1} (60 mL); 30°C	96	68.64	[23]
Carbon/Fe	Dosage: 0.1 g L^{-1}; H_2O_2: 6 mM; pH: 3; Orange II: 0.1 mM (1 L); 30°C	100	350.32	[24]
Vanadium-titanium magnetite	Dosage: 1.0 g L^{-1}; H_2O_2: 10 mM; pH: 3; Orange II: 02 mM (200 mL); 30°C	100	70.00	[25]
Al-pillared Fe-smectite	Dosage: 0.5 g L^{-1}; H_2O_2: 13.5 mM; pH: 3; Orange II: 80 mg L^{-1} (100 mL); 25°C	88	160.00	[26]
Fe_3O_4@g-Fe_2O_3	Dosage: 1.0 g L^{-1}; H_2O_2: 10 mM; pH: 3; Orange II: 70 mg L^{-1} (354 mL); 25°C	100	70.00	[27]

0.20~1.20 g. This could be attributed to the fact that the excess Fe^0 could produce excess Fe^{2+}, which reacted with hydroxyl radicals as a radical scavenger (Eq. (3)) [32].

$$Fe^{2+} + OH^{\bullet} \rightarrow Fe^{3+} + OH^- \quad (3)$$

The effect of H_2O_2 concentration in the range from 10 to 900 mM was investigated. Fig. 4 indicates that the removal efficiency of Orange II increased as a result of the increase in H_2O_2 concentration from 10 to 100 mM while the increase in H_2O_2 concentration from 300 to 900 mM had an adverse effect on the removal of Orange II. More hydroxyl radicals were generated in the GPA-ZVI/H_2O_2 system via H_2O_2 reacting with Fe^{2+} as the H_2O_2 concentration increased, resulting in increasing the removal efficiency of Orange II. However, an excess H_2O_2 concentration had an adverse influence on Orange II removal. The reason for this was that hydroxyl radicals could be depleted through the scavenging of hydroxyl radicals by excess H_2O_2 when H_2O_2 concentration exceeded a critical concentration in the GPA-ZVI/H_2O_2 system (Eqs. (4) and (5)) [33].

$$H_2O_2 + OH^{\bullet} \rightarrow H_2O + HO_2 \quad (4)$$

$$OH^{\bullet} + HO_2^{\bullet} \rightarrow H_2O + O_2 \quad (5)$$

The effect of temperature in the range from 293 to 313 K on Orange II removal was studied. Fig. 5 shows that the removal efficiency of Orange II increased from 85.35% to 99.93% with an increase in the temperature from 293 to 313 K. This could be explained by the acceleration of the corrosion of Fe^0 into Fe^{2+} and the decomposition of H_2O_2 into hydroxyl radicals at higher temperature, which led to the increase in the removal of Orange II. Furthermore, a higher temperature enhanced the collision frequency between Orange II and hydroxyl radicals, leading to a rapid removal rate. However, the removal efficiency decreased from 99.93% to 93.37% as the temperature rose from 313 to 323 K. This could be attributed to the acceleration in the thermal decomposition of H_2O_2 into oxygen and water, which leads to a scavenging effect [34].

Although the Fenton process could efficiently remove Orange II, excess H_2O_2 and GPA-ZVI dosage would reduce

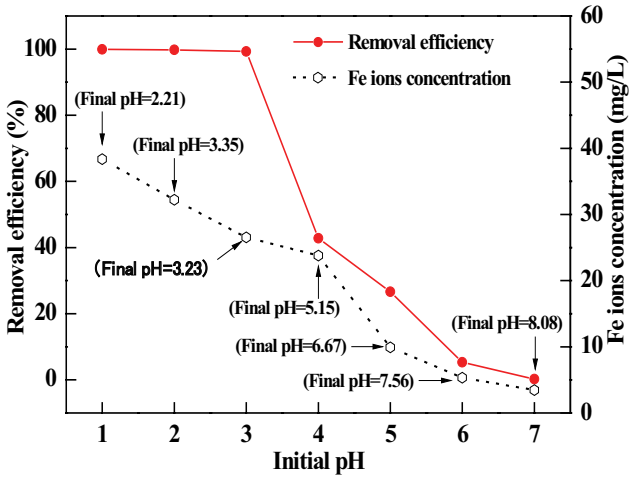

Fig. 2. Effect of pH on the removal efficiency of Orange II (Initial Orange II concentration 1,000 mg L^{-1}, H_2O_2 concentration 50 mM, catalyst dosage 2 g L^{-1}, pH 1~7, temperature 303 K).

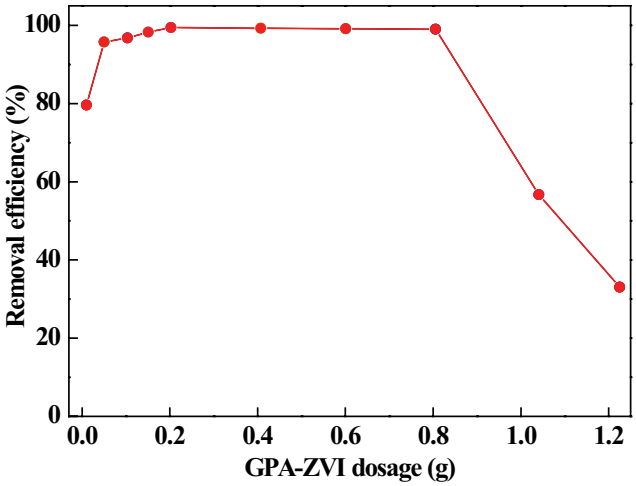

Fig. 3. GPA-ZVI dosage on the removal efficiency of Orange II (Initial Orange II concentration 1,000 mg L^{-1}, H_2O_2 concentration 50 mM, catalyst dosage 0.1~12 g L^{-1}, pH 3, temperature 303 K).

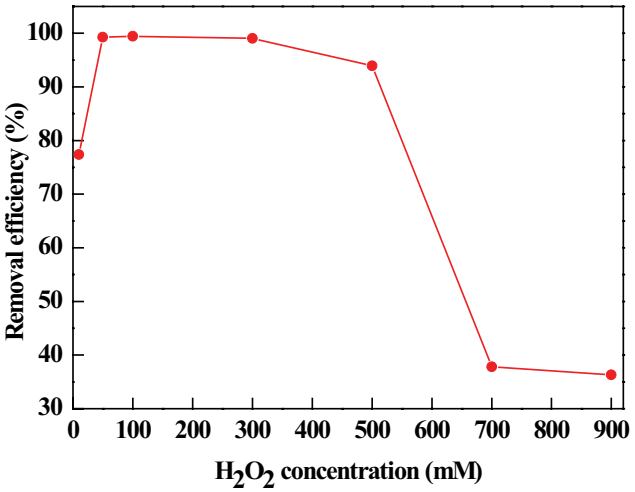

Fig. 4. H_2O_2 concentration on the removal efficiency of Orange II (Initial Orange II concentration 1,000 mg L^{-1}, H_2O_2 concentration 10~900 mM, catalyst dosage 2 g L^{-1}, pH 3, temperature 303 K).

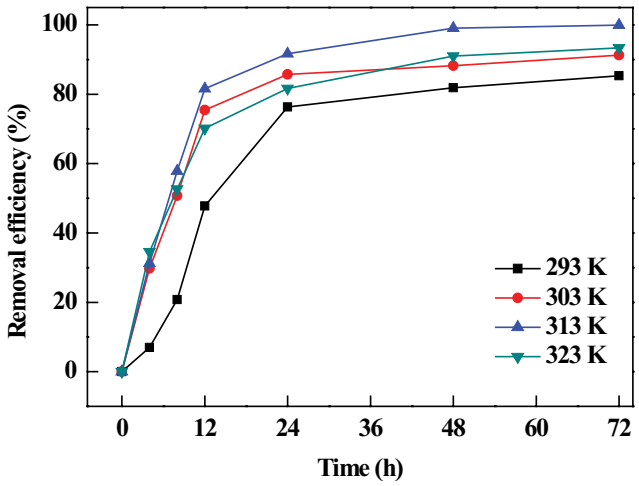

Fig. 5. Reaction temperature on the removal efficiency of Orange II (Initial Orange II concentration 1,000 mg L^{-1}, H_2O_2 concentration 50 mM, catalyst dosage 2 g L^{-1}, pH 3, temperature 293~323 K).

the removal efficiency, leading to the high cost of wastewater treatment. Therefore, it was necessary to optimize the adding amount of H_2O_2 and GPA-ZVI according to the initial concentration of Orange II. When the initial concentration of Orange II was 1,000 mg L^{-1}, the pH of 3, GPA-ZVI dosage of 0.2 g, H_2O_2 concentration of 50 mM and temperature of 313 K were the best choice.

3.4. Degradation kinetics

The pseudo-first-order reaction model and the pseudo-second-order reaction model were utilized to study the removal mechanism of Orange II by GPA-ZVI/H_2O_2.

The pseudo-first-order equation was described as below [5]:

$$\ln\frac{C_t}{C_0} = -k_{obs1}t \tag{6}$$

where C_0 (mg L^{-1}) is the initial concentration, k_{obs1} (h^{-1}) is the pseudo-first-order rate constant, C_t (mg L^{-1}) is the concentration at time t.

The Arrhenius equation was described as below [35]:

$$\ln k_{obs1} = -\frac{E_a}{RT} + \ln A_0 \tag{7}$$

where E_a (kJ mol^{-1}) is the Arrhenius activation energy, R is the ideal gas constant, A_0 is the pre-exponential factor, T (K) is the temperature.

The pseudo-second-order model equation was presented as below [36]:

$$\ln\left(\frac{1}{C_t} - \frac{1}{C_0}\right) = k_{obs2}t \tag{8}$$

where k_{obs2} (h^{-1}) is the pseudo-second-order reaction rate constant.

The removal of Orange II by GPA-ZVI/H_2O_2 at different temperatures and Orange II concentration was studied and the results of the kinetics analysis are listed in Table 2. The degradation of Orange II could be fitted with the pseudo-first-order kinetic model according to the value of R^2. The removal rate constant decreased from 0.0377 to 0.0183 h^{-1} with an increase in the Orange II concentration ranged from 200 to 1,000 mg L^{-1}, which indicated that the removal rate was related to adsorption sites on the surface of GPA-ZVI

Table 2
Degradation kinetics parameters of Orange II by GPA-ZVI/H_2O_2

T (K)	C (mg L^{-1})	Pseudo-first-order model		Pseudo-second-order model	
		R^2	k_{obs1} (h^{-1})	R^2	k_{obs2} (h^{-1})
303	200	0.9972	0.0377	0.9005	0.2917
303	600	0.9631	0.0228	0.9202	0.2956
303	1,000	0.9579	0.0183	0.8908	0.2865
293	1,000	0.9582	0.0177	0.8760	0.3576
303	1,000	0.9579	0.0183	0.8908	0.2865
313	1,000	0.9501	0.0215	0.8557	0.2715

and the Orange II concentration [37]. On the other hand, the removal rate increased from 0.0177 to 0.0215 h^{-1} as the temperature increased from 293 to 313 K, which demonstrated that a higher temperature enhanced the reactivity and the removal process of Orange II by GPA-ZVI/H_2O_2 was endothermic [38]. The Arrhenius activation energy of Orange II removal by GPA-ZVI/H_2O_2 was 7.36 kJ mol^{-1} [39].

3.5. Possible removal mechanism in Fenton-like system

Based on the previous literature, the removal mechanism of Orange II by GPA-ZVI/H_2O_2 included the dominating oxidization of Orange II by hydroxyl radicals and the adsorption of Orange II onto GPA-ZVI [40–42]. The steps of Orange II removal by GPA-ZVI/H_2O_2 were as follows (Fig. 6): (i) Firstly, the Orange II molecules were adsorbed onto GPA-ZVI, (ii) ZVI on the surface of GPA-ZVI was converted to Fe^{2+} under an acidic condition for activating H_2O_2 to produce hydroxyl radicals, and (iii) Subsequently, the Orange II molecules were oxidized to the products by hydroxyl radicals generated in the existence of H_2O_2 and Fe^{2+} from the corrosion of ZVI [15].

To further study the possible removal process, the UV-vis spectra of the Orange II were recorded in the range from 190 to 1,100 nm at different reaction times in the presence of GPA-ZVI/H_2O_2 or GAP-ZVI alone as depicted in Figs. 7a and b. The characteristic peaks of Orange II were 484, 310, and 230 nm, which were ascribed to azo bond, a naphthalene ring and a benzene ring. Fig. 7a shows that the absorbance band at 230, 310, and 484 nm decreased with reaction times, indicating the destruction of the naphthyl, benzene rings, and the cleavage of the azo bonds. It was also observed that the color of the solution changed from orange to dark to brown [43,44]. Based on the previous literature, the removal of Orange II by hydroxyl radicals firstly occurred via the cleavage of the azo bond to sulfanilic acid and 1-amino-2-naphthol [4,45]. Finally, Orange II was degraded to CO_2, H_2O, and some other products (Fig. 8). Fig. 7a shows that the peak at about 210 nm in the UV-vis spectra of the Orange II in the presence of GPA-ZVI/H_2O_2 became stronger and afterward disappeared after the reaction, demonstrating that the new products were formed and afterward they were degraded. Also, it is seen from Fig. 7b that the absorbance band in the UV-vis spectra of the Orange II in the presence of GPA-ZVI decreased with reaction time, meaning that Orange II could be removed by GPA-ZVI and adsorbed onto GPA-ZVI. It indicated that the adsorption was one of the removal mechanisms of Orange II by GPA-ZVI/H_2O_2.

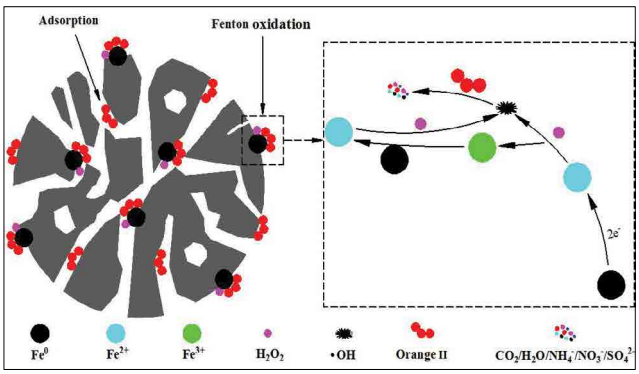

Fig. 6. Schematic diagram of Orange II removal processes by GPA-ZVI/H_2O_2.

To further probe the degradation mechanisms of Orange II by GPA-ZVI/H_2O_2, the chemical structure of GPA-ZVI before and after the experiment was investigated via XRD analysis. As can be seen from Fig. 9, the characteristic peak of ZVI at 44.9° is found to be weakened for GPA-ZVI after the reaction, which indicated that ZVI was converted to Fe^{2+} and Fe^{3+} ions in the Fenton oxidation process. Subsequently, Fe^{2+} and Fe^{3+} ions were adsorbed onto the surface of GPA-ZVI. Furthermore, the intensities of the peaks of Fe_2O_3, Fe_3O_4 slightly strengthened, demonstrating that Fe^{2+} and Fe^{3+} ions formed Fe_2O_3, Fe_3O_4, and $Fe(OH)_3$ precipitates on the surface of GPA-ZVI [46].

4. Conclusions

In this paper, GPA-ZVI was prepared and the application of GPA-ZVI as a Fenton-like catalyst for removing Orange II was investigated at various conditions. The characterization

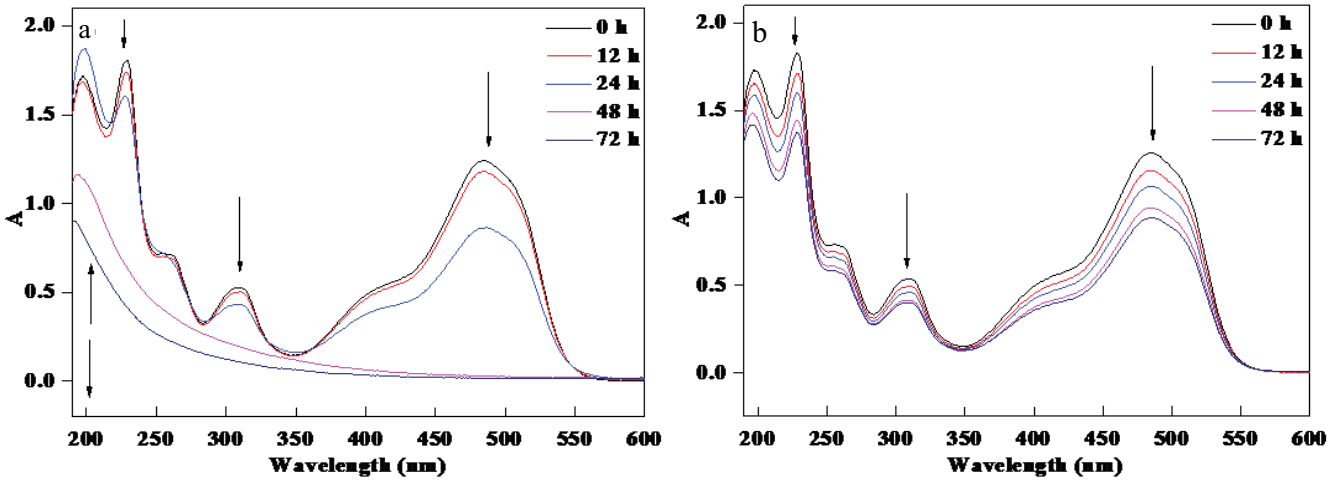

Fig. 7. UV-vis spectra of Orange II at various times in the presence of (a) GPA-ZVI/H_2O_2 and (b) GPA-ZVI.

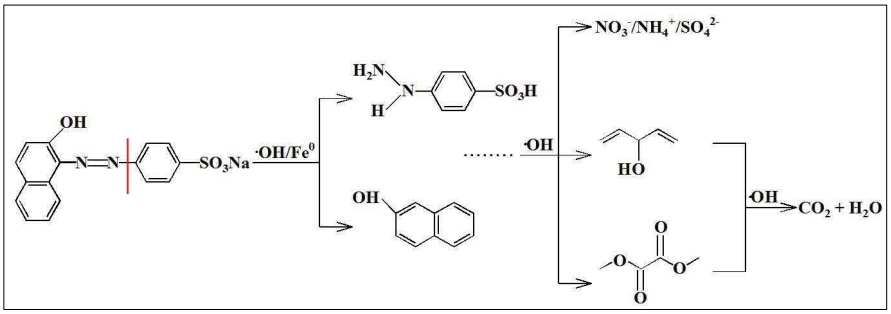

Fig. 8. Possible pathways for the degradation of Orange II [26].

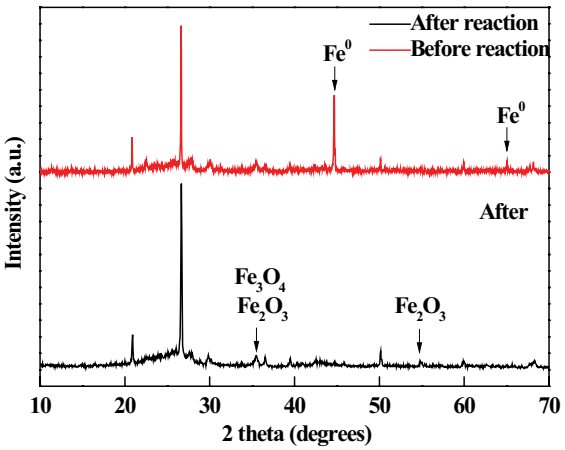

Fig. 9. XRD patterns of GPA-ZVI before and after reactions.

of GPA-ZVI by SEM, EDS, XRD, FTIR, and BET revealed that GPA-ZVI was a porous adsorbent owning various functional groups and ZVI was evenly distributed in GPA-ZVI as a support material. The initial pH value of the solution, H_2O_2 concentration, GPA-ZVI dosage and temperature greatly affected the removal efficiency of Orange II. The results showed 91.24% degradation of 1,000 mg L^{-1} Orange II using GPA-ZVI/H_2O_2. The removal of Orange II by GPA-ZVI/H_2O_2 followed the pseudo-first-order kinetic model. The removal mechanism of Orange II by GPA-ZVI/H_2O_2 included the dominating oxidization of Orange II by hydroxyl radicals and the adsorption of Orange II onto the surface of GPA-ZVI. In a word, GPA-ZVI/H_2O_2 demonstrated a high-efficiency method for the degradation of Orange II.

Acknowledgments

The authors acknowledge the support of the State Key Laboratory of Environmental Criteria and Risk Assessment (SKLECRA2013FP12) and the Shandong Province Key Research and Development Program (2016GSF115040).

References

[1] C.Q. Zhang, Z.W. Zhu, H.F. Zhang, Z.Q. Hu, Rapid decolorization of Acid Orange II aqueous solution by amorphous zero-valent iron, J. Environ. Sci., 24 (2012) 1021–1026.
[2] C. He, J.N. Yang, L.F. Zhu, Q. Zhang, W.C. Liao, S.K. Liu, Y. Liao, M.A. Asi, D. Shu, pH-dependent degradation of acid orange II by zero-valent iron in presence of oxygen, Sep. Purif. Technol., 117 (2013) 59–68.
[3] S. Shakoor, A. Nasar, Removal of methylene blue dye from artificially contaminated water using citrus limetta peel waste as a very low cost adsorbent, J. Taiwan Inst. Chem. Eng., 66 (2016) 154–163.
[4] S. Luo, P.F. Qin, J.H. Shao, L. Peng, Q.R. Zeng, J.-D. Gu, Synthesis of reactive nanoscale zero valent iron using rectorite supports and its application for Orange II removal, Chem. Eng. J., 223 (2013) 1–7.
[5] J. Lin, M. Sun, X. Liu, Z. Chen, Functional kaolin supported nanoscale zero-valent iron as a Fenton-like catalyst for the degradation of Direct Black G, Chemosphere, 184 (2017) 664–672.
[6] G. Vilardi, J.M. Ochando-Pulido, N. Verdone, M. Stoller, L.D. Palma, On the removal of hexavalent chromium by olive stones coated by iron-based nanoparticles: equilibrium study and chromium recovery, J. Cleaner Prod., 190 (2018) 200–210.
[7] Y. Segura, F. Martínez, J.A. Melero, J.L.G. Fierro, Zero valent iron (ZVI) mediated Fenton degradation of industrial wastewater: treatment performance and characterization of final composites, Chem. Eng. J., 269 (2015) 298–305.
[8] S. Ambika, M. Devasena, I.M. Nambi, Synthesis, characterization and performance of high energy ball milled meso-scale zero valent iron in Fenton reaction, J. Environ. Manage., 181 (2016) 847–855.
[9] G. Vilardi, J.M. Ochando-Pulido, M. Stoller, N. Verdone, L. Di Palma, Fenton oxidation and chromium recovery from tannery wastewater by means of iron-based coated biomass as heterogeneous catalyst in fixed-bed columns, Chem. Eng. J., 351 (2018) 1–11.
[10] M. Kallel, C. Belaid, R. Boussahel, M. Ksibi, A. Montiel, B. Elleuch, Olive mill wastewater degradation by Fenton oxidation with zero-valent iron and hydrogen peroxide, J. Hazard. Mater., 163 (2009) 550–554.
[11] J.A. Donadelli, L. Carlos, A. Arques, F.S.G. Einschlag, Kinetic and mechanistic analysis of azo dyes decolorization by ZVI-assisted Fenton systems: pH-dependent shift in the contributions of reductive and oxidative transformation pathways, Appl. Catal., B, 231 (2018) 51–61.
[12] N. Jaafarzadeh, A. Takdastan, S. Jorfi, F. Ghanbari, M. Ahmadi, G. Barzegar, The performance study on ultrasonic/Fe_3O_4/H_2O_2 for degradation of azo dye and real textile wastewater treatment, J. Mol. Liq., 256 (2018) 462–470.
[13] R. Cheng, C. Cheng, G.-H. Liu, X. Zheng, G.Q. Li, J. Li, Removing pentachlorophenol from water using a nanoscale zero-valent iron/H_2O_2 system, Chemosphere, 141 (2015) 138–143.
[14] A. Shimizu, M. Tokumura, K. Nakajima, Y. Kawase, Phenol removal using zero-valent iron powder in the presence of dissolved oxygen: roles of decomposition by the Fenton reaction and adsorption/precipitation, J. Hazard. Mater., 201 (2012) 60–67.
[15] H.-J. Fan, S.-T. Huang, W.-H. Chung, J.-L. Jan, W.-Y. Lin, C.-C. Chen, Degradation pathways of crystal violet by

Fenton and Fenton-like systems: condition optimization and intermediate separation and identification, J. Hazard. Mater., 171 (2009) 1032–1044.
[16] Y. Man, J.-X. Feng, Effect of iron ore-coal pellets during reduction with hydrogen and carbon monoxide, Powder Technol., 301 (2016) 1213–1217.
[17] J.X. Zhang, B.H. Jiang, D. Wang, Thermogravimetric and kinetic analysis of bio-crude from hydrothermal liquefaction of *Enteromorpha prolifera*, Algal Res., 18 (2016) 45–50.
[18] N. Arancibia-Miranda, S.E. Baltazar, A. García, D. Muñoz-Lira, P. Sepúlveda, M.A. Rubio, D. Altbir, Nanoscale zero valent supported by Zeolite and Montmorillonite: template effect of the removal of lead ion from an aqueous solution, J. Hazard. Mater., 301 (2016) 371–380.
[19] C. Jiao, Y. Cheng, W. Fan, J. Li, Synthesis of agar-stabilized nanoscale zero-valent iron particles and removal study of hexavalent chromium, Int. J. Environ. Sci. Technol., 12 (2015) 1603–1612.
[20] N. Inchaurrondo, J. Font, C.P. Ramos, P. Haure, Natural diatomites: efficient green catalyst for Fenton-like oxidation of Orange II, Appl. Catal., B, 181 (2016) 481–494.
[21] T. Shahwan, S.A. Sirriah, M. Nairat, E. Boyacı, A.E. Eroğlu, T.B. Scott, K.R. Hallam, Green synthesis of iron nanoparticles and their application as a Fenton-like catalyst for the degradation of aqueous cationic and anionic dyes, Chem. Eng. J., 172 (2011) 258–266.
[22] B.-H. Moon, Y.-B. Park, K.-H. Park, Fenton oxidation of Orange II by pre-reduction using nanoscale zero-valent iron, Desalination, 268 (2011) 249–252.
[23] S.H. Tian, Y.T. Tu, D.S. Chen, X. Chen, Y. Xiong, Degradation of Acid Orange II at neutral pH using $Fe_2(MoO_4)_3$ as a heterogeneous Fenton-like catalyst, Chem. Eng. J., 169 (2011) 31–37.
[24] F. Duarte, F.J. Maldonado-Hódar, L.M. Madeira, New insight about Orange II elimination by characterization of spent activated carbon/Fe Fenton-like catalysts, Appl. Catal., B, 129 (2013) 264–272.
[25] X.L. Liang, Y.H. Zhong, S.Y. Zhu, J.X. Zhu, P. Yuan, H.P. He, J. Zhang, The decolorization of Acid Orange II in non-homogeneous Fenton reaction catalyzed by natural vanadium–titanium magnetite, J. Hazard. Mater., 181 (2010) 112–120.
[26] H.Y. Li, Y.L. Li, L.J. Xiang, Q.Q. Huang, J.J. Qiu, H. Zhang, M.V. Sivaiah, F. Baron, J. Barrault, S. Petit, S. Valange, Heterogeneous photo-Fenton decolorization of Orange II over Al-pillared Fe-smectite: response surface approach, degradation pathway, and toxicity evaluation, J. Hazard. Mater., 287 (2015) 32–41.
[27] H.W. Dai, S.Y. Xu, J.X. Chen, X.Z. Miao, J.X. Zhu, Oxalate enhanced degradation of Orange II in heterogeneous UV-Fenton system catalyzed by Fe_3O_4@γ-Fe_2O_3 composite, Chemosphere, 199 (2018) 147–153.
[28] M. Kallel, C. Belaid, T. Mechichi, M. Ksibi, B. Elleuch, Removal of organic load and phenolic compounds from olive mill wastewater by Fenton oxidation with zero-valent iron, Chem. Eng. J., 150 (2009) 391–395.
[29] G.B.O. de la Plata, O.M. Alfano, A.E. Cassano, 2-Chlorophenol degradation via photo Fenton reaction employing zero valent iron nanoparticles, J. Photochem. Photobiol., A, 233 (2012) 53–59.
[30] L. Wang, J. Yang, Y.M. Li, J. Lv, J. Zou, Removal of chlorpheniramine in a nanoscale zero-valent iron induced heterogeneous Fenton system: influencing factors and degradation intermediates, Chem. Eng. J., 284 (2016) 1058–1067.
[31] C.-H. Weng, Y.-T. Lin, C.-K. Chang, N. Liu, Decolourization of direct blue 15 by Fenton/ultrasonic process using a zero-valent iron aggregate catalyst, Ultrason. Sonochem., 20 (2013) 970–977.
[32] J.Y. Shen, C.J. Ou, Z.Y. Zhou, J. Chen, K.X. Fang, X.Y. Sun, J.S. Li, L. Zhou, L.J. Wang, Pretreatment of 2,4-dinitroanisole (DNAN) producing wastewater using a combined zero-valent iron (ZVI) reduction and Fenton oxidation process, J. Hazard. Mater., 260 (2013) 993–1000.
[33] Y. Segura, F. Martínez, J.A. Melero, Effective pharmaceutical wastewater degradation by Fenton oxidation with zero-valent iron, Appl. Catal., B, 136–137 (2013) 64–69.
[34] B. Yang, Z. Tian, L. Zhang, Y.P. Guo, S.Q. Yan, Enhanced heterogeneous Fenton degradation of Methylene Blue by nanoscale zero valent iron (nZVI) assembled on magnetic Fe_3O_4/reduced graphene oxide, J. Water Process Eng., 5 (2015) 101–111.
[35] Q.X. Xia, Z.H. Jiang, J.K. Wang, Z.P. Yao, A facile preparation of hierarchical dendritic zero-valent iron for Fenton-like degradation of phenol, Catal. Commun., 100 (2017) 57–61.
[36] S.X. Zha, Y. Cheng, Y. Gao, Z.L. Chen, M. Megharaj, R. Naidu, Nanoscale zero-valent iron as a catalyst for heterogeneous Fenton oxidation of amoxicillin, Chem. Eng. J., 255 (2014) 141–148.
[37] F. Luo, D. Yang, Z. Chen, M. Megharaj, R. Naidu, One-step green synthesis of bimetallic Fe/Pd nanoparticles used to degrade Orange II, J. Hazard. Mater., 303 (2016) 145–153.
[38] Z. Chen, T. Wang, X. Jin, Z. Chen, M. Megharaj, R. Naidu, Multifunctional kaolinite-supported nanoscale zero-valent iron used for the adsorption and degradation of crystal violet in aqueous solution, J. Colloid Interface Sci., 398 (2013) 59–66.
[39] X. Wang, A. Wang, J. Ma, M. Fu, Facile green synthesis of functional nanoscale zero-valent iron and studies of its activity toward ultrasound-enhanced decolorization of cationic dyes, Chemosphere, 166 (2017) 80–88.
[40] F. Luo, D. Yang, Z.L. Chen, M. Megharaj, R. Naidu, The mechanism for degrading Orange II based on adsorption and reduction by ion-based nanoparticles synthesized by grape leaf extract, J. Hazard. Mater., 296 (2015) 37–45.
[41] A.N. Soon, B.H. Hameed, Heterogeneous catalytic treatment of synthetic dyes in aqueous media using Fenton and photo-assisted Fenton process, Desalination, 269 (2011) 1–16.
[42] I. Grčić, S. Papić, K. Žižek, N. Koprivanac, Zero-valent iron (ZVI) Fenton oxidation of reactive dye wastewater under UV-C and solar irradiation, Chem. Eng. J., 195–196 (2012) 77–90.
[43] H. Barndõk, L. Blanco, D. Hermosilla, Á. Blanco, Heterogeneous photo-Fenton processes using zero valent iron microspheres for the treatment of wastewaters contaminated with 1,4-dioxane, Chem. Eng. J., 284 (2016) 112–121.
[44] G.M.S. Elshafei, F.Z. Yehia, Gh. Eshaq, A.E. Elmetwally, Enhanced degradation of nonylphenol at neutral pH by ultrasonic assisted-heterogeneous Fenton using nano zero valent metals, Sep. Purif. Technol., 178 (2017) 122–129.
[45] F.M. Duarte, F.J. Maldonado-Hódar, L.M. Madeira, Influence of the iron precursor in the preparation of heterogeneous Fe/activated carbon Fenton-like catalysts, Appl. Catal., A, 458 (2013) 39–47.
[46] S. Ambika, M. Devasena, I.M. Nambi, Assessment of meso scale zero valent iron catalyzed Fenton reaction in continuous-flow porous media for sustainable groundwater remediation, Chem. Eng. J., 334 (2017) 264–272.

Supplementary information

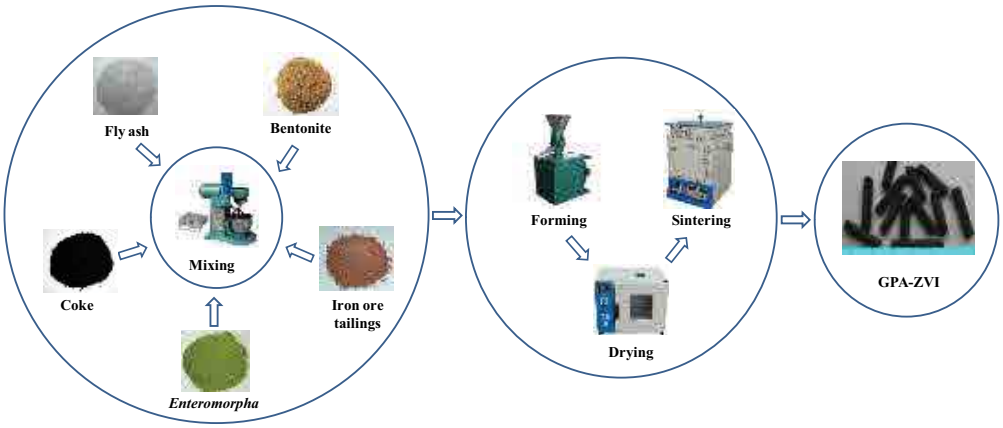

Fig. S1. Schematic diagram of GPA-ZVI preparation.

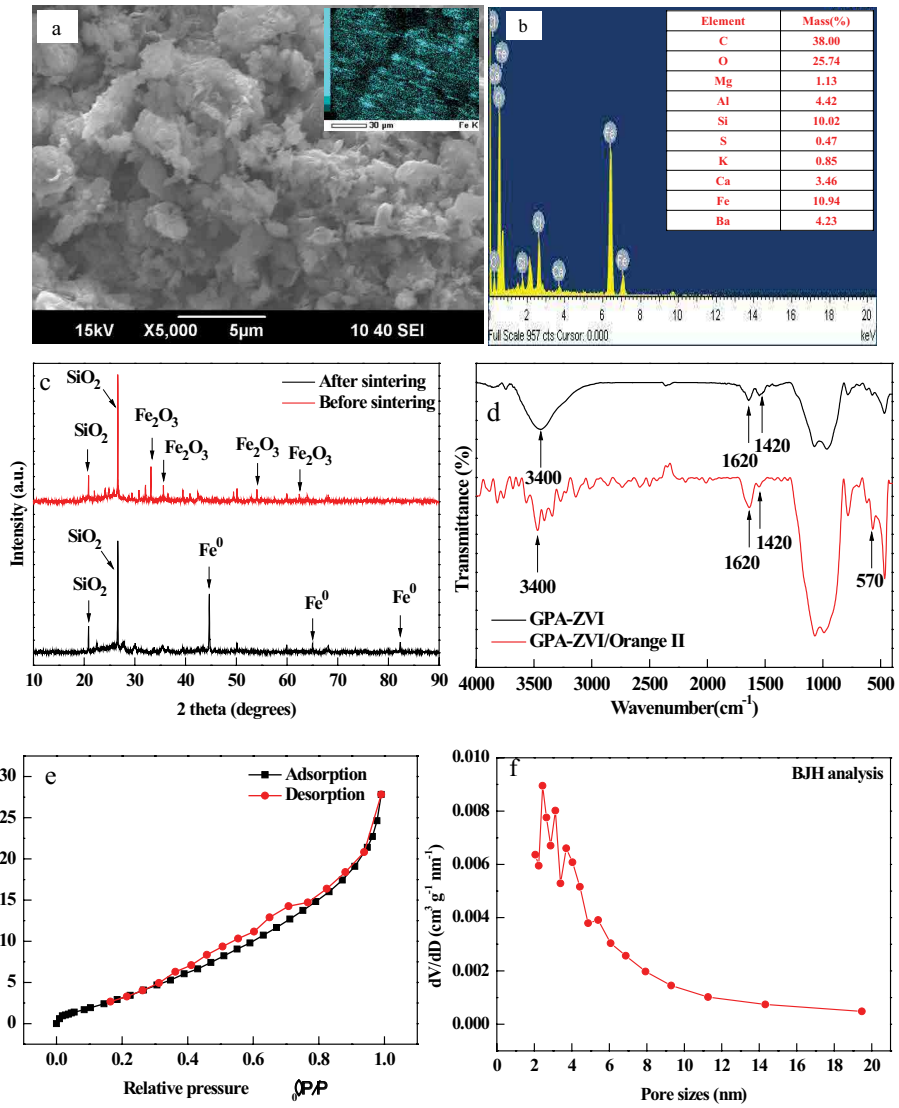

Fig. S2. (a) SEM image of GPA-ZVI, (b) EDX image of GPA-ZVI, (c) XRD pattern of GPA-ZVI before and after sintering, (d) FTIR spectra of GPA-ZVI before and after reactions with Orange II, (e) Nitrogen adsorption-desorption isotherm of GPA-ZVI, and (f) Pore size distribution of GPA-ZVI.